Use of Cross-Links To Study the Conformational Dynamics of Triplex DNA†

Robert J. Cain‡ and Gary D. Glick*

Department of Chemistry, University of Michigan, Ann Arbor, Michigan 48109-1055

Received June 5, 1997; Revised Manuscript Received September 18, 1997

ABSTRACT: The conformational dynamics of a 34-base-long pyrimidine·purine-pyrimidine motif intramolecular DNA triple helix possessing three cytosine residues in the Hoogsteen strand (**1**) and a disulfide cross-linked analog (**2**) were studied by two-dimensional exchange and NOE spectroscopy and by measuring base-catalyzed imino proton exchange rates. Under acidic conditions that stabilize triplexes containing Hoogsteen strand cytosines (pH 6.0 and 1 °C), sequences **1** and **2** exhibit a small and identical degree of conformational heterogeneity. However, at a higher temperature (pH 6.0 and 37 °C), **1** exhibits much more extensive conformational heterogeneity than **2**. The exchange times for Watson−Crick imino protons are ∼1 h for both triplexes. However, the Hoogsteen base-pair lifetimes of **1** could not be measured because this sequence is conformationally labile under the alkaline conditions necessary to conduct these experiments. Because of the extraordinary pH stability conferred by the cross-link, it is possible to estimate the base-pair lifetimes for **2**. The lifetimes of the Hoogsteen base pairs range from about 3 to 370 ms, and in all cases are shorter than that of the Watson−Crick base pair contained in the same triplet. These experiments represent the first measurement of base-pair lifetimes within Hoogsteen triplets. The ability to measure individual base-pair lifetimes may prove useful in studies that attempt to modulate triplex properties through rational design.

DNA triple helices can form when a third strand binds in the major groove of duplex DNA via Hoogsteen base pairing (Felsenfeld et al., 1957; Dervan, 1992; Plum et al., 1995; Soyfer & Potaman, 1996; Thuong & Hélène, 1993; Sun et al., 1996). Triple helices have generated considerable interest because their existence in vivo has led to speculation and research into possible biological roles for this structural motif (Mirkin & Frank-Kamenetskii, 1994). In addition, sequence specific recognition can be achieved by designing oligonucleotides that bind in the major groove of duplex DNA forming either pyr·pur-pyr[1,2] or pur·pur-pyr triple helices (Moser & Dervan, 1987). This recognition is a powerful tool in a number of laboratory and diagnostic protocols and could have implications for antigene therapeutics (Heider & Bardos, 1995). The affinity and specificity of third strand binding are effected by a number of factors such as sequence length (i.e., the number of triplets formed), composition, and the presence of base-pair mismatches, as well as solution conditions, including pH and mono- and divalent counterion concentrations (Soyfer & Potaman, 1996). For example, a major factor in the stability of triplexes that contain C^+·G-C triplets is the necessity of protonation of the N_3 position of cytosine, which generally limits the stability of small triple helices of this type to pH <7 (Singleton & Dervan, 1992).

While a significant body of data exists describing the "static" structure of triplex DNA (Radhakrishnan et al., 1991; Radhakrishnan & Patel, 1993, 1994a; Macaya et al., 1992) and its water-binding properties (Radhakrishnan & Patel, 1994b,c), relatively little is known regarding the conformational dynamics of this motif. On a fundamental level, such information will contribute to our understanding of the factors that stabilize Watson−Crick and non-Watson−Crick structures, and practically may aid in the design of oligonucleotides for binding duplexes both in vitro and in vivo, and may also be helpful in understanding the biological role of triplexes (Plum et al., 1995). Here, we present the results of NMR experiments designed to investigate the internal dynamics of an intramolecular triple helix, **1**, and a disulfide-stabilized analog **2** (Figure 1). These experiments represent the first measurement of base-pair lifetimes within Hoogsteen base-pair triplets and were only possible because the disulfide cross-link in sequence **2** confers unprecedented pH and thermal stability relative to the parent triplex and other sequences containing C^+·G-C triplets (Osborne et al., 1997; Völker et al., 1997).

MATERIALS AND METHODS

Materials. Triplex samples were synthesized and purified as described previously (Osborne et al., 1997). For NMR

† This research was supported by National Institutes of Health Grant GM 52831. G.D.G. is the recipient of an American Cancer Society Junior Faculty Research Award, a National Science Foundation Young Investigator Award, a Camille Dreyfus Teacher-Scholar Award, and a Research Fellowship from the Alfred P. Sloan Foundation.

* Author to whom correspondence should be addressed. Phone: (313) 764-4548. Fax: (313) 764-8815. E-mail: gglick@umich.edu.

‡ Present address: Department of Biochemistry, North Carolina State University, Raleigh, NC 27695-7622.

[1] Abbreviations: dA, 2′-deoxyadenosine; dC, 2′-deoxycytosine; dG, 2′-deoxyguanine; dT, 2′-deoxythymidine; I-BURP, band-selective uniform response pure-phase inversion pulse; NMR, nuclear magnetic resonance; NOE, nuclear Overhauser effect; NOESY, nuclear Overhauser effect spectroscopy; PBS, phosphate-buffered saline [NaCl (8 g), KCl (0.2 g), Na_2HPO_4 (1.44 g), and KH_2PO_4 (0.24 g) in H_2O (1 L)]; pur, purine; pyr, pyrimidine; TPPI, time-proportional phase incrementation; TRIS, tris(hydroxymethyl)aminomethane; UV, ultraviolet.

[2] Hoogsteen base pairing is signified with a dot (·), and Watson−Crick base pairing is designated with a dash (−).

S0006-2960(97)01342-1 CCC: $15.00
Published on Web 01/13/1998

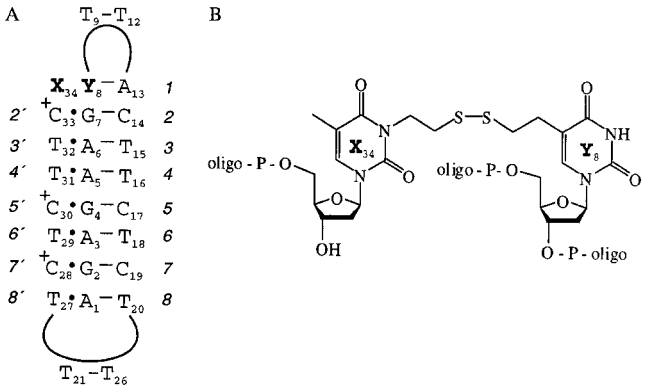

FIGURE 1: Triplex base-pairing scheme and the chemical structure of the cross-link. (A) Watson−Crick base pairs are represented with dashes (−), and Hoogsteen base pairs are represented with dots (·). The numbering schemes for the Watson−Crick and the Hoogsteen base pairs and imino protons are indicated in italics to the right and left of the structure, respectively. Thus, the Hoogsteen base pair dT31·dA5 is referred to as base pair 4′. This numbering scheme is used throughout the text. For **1**, X34 and Y8 are both thymidine residues. (B) Chemical structure of the cross-link.

experiments that did not use added exchange catalyst, DNA samples were dissolved in PBS (500 μL) containing $MgCl_2$ (0.5 mM) and 10% D_2O. The pH was adjusted in the NMR tube with either HCl (1 N) or NaOH (1 N). For the samples containing exchange catalyst, TRIS buffer concentrations were varied by addition of a stock solution of TRIS (0.93 M) in NaCl (50 mM), EDTA (2 mM), and 10% D_2O. Between additions of the stock solution, the sample was lyophilized to maintain a constant solution volume. The pH was adjusted to 7.8 ± 0.05 with NaOH (1 N) or HCl (1 N) and measured with a microelectrode (Microelectrodes, Inc., MI-412) inside the NMR tube at 22.4 °C before and after each NMR experiment. The concentration of the unprotonated, exchange catalyst form of TRIS, [cat], was calculated according to

$$[\mathrm{cat}] = [\mathrm{B}]/[1 + 10^{(\mathrm{p}K_a - \mathrm{pH})}] \quad (1)$$

where [B] is the total TRIS concentration and the pK_a of the TRIS was determined by titration at 22.4 °C (Cain & Glick, 1997). The variation of pH with temperature was calculated according to a TRIS pK_a change of −0.031 ΔpK_a unit/°C. Thus, T_1 measurements, measured in TRIS buffer at 4, 21, and 38 °C, reflect pH values of ca. 8.4, 7.8, and 7.3, respectively.

NMR Spectroscopy. NMR spectra were measured on a Bruker AMX 500 spectrometer. The data were transferred to a Silicon Graphics workstation and processed using FELIX software (Biosym Technologies). The H_2O signal was suppressed using a 1-1 read pulse in all experiments (Plateau & Guéron, 1982). NOESY spectra (τ_m = 100 ms, TPPI phase cycling) were measured with a homospoil pulse (10 ms) inserted into the mixing time to alleviate radiation damping (Ernst et al., 1987). The proton longitudinal relaxation times were measured using the inversion recovery technique. An I-BURP pulse (4 ms) was used for the selective inversion of the imino protons (Geen & Freeman, 1991). A spectral width of 25 000 Hz was used to achieve the flattest baselines which were necessary for the subsequent peak fitting procedure. For each T_1 measurement, 13−20 values for the recovery delay were used.

The intensities at each delay time were measured by fitting the spectra to a set of Lorentzian peaks. For each inversion recovery series, the spectrum measured using the longest delay time was fit first. The line widths and peak positions were then held constant in subsequently fitting peaks to the spectra measured with shorter delay times. As the catalyst concentrations were increased, some resonances became significantly exchange broadened, making it impossible to measure the longitudinal relaxation times of some of the fast exchanging resonances at high exchange catalyst concentrations.

The exchange times due to added catalyst were determined according to the equation

$$1/T_1 = 1/\tau_{ex} + 1/T_{1aac} \quad (2)$$

where T_1 is the longitudinal relaxation time measured at a given catalyst concentration, T_{1aac} is the longitudinal relaxation time measured without any added exchange catalyst, and τ_{ex} is the proton exchange time at the given catalyst concentration (Günther, 1995). This technique is useful for determining exchange lifetimes that do not greatly exceed T_{1aac}. The lifetimes of individual base pairs were determined by fitting plots of τ_{ex} versus 1/[cat] to a straight line, as described below.

For real-time exchange experiments, the samples were first equilibrated under the desired solution conditions and then lyophilized and dissolved in H_2O (50 μL) and inserted into an NMR tube. The sample and a pipette containing D_2O (450 μL) were then cooled in an ice bath. Immediately before the NMR experiment was started, the D_2O was injected into the sample to effect mixing. Spectra were collected continuously until the samples were fully exchanged. After normalization for the number of scans, the fully exchanged spectrum was subtracted from the spectra acquired previously. The peaks were then quantitated by fitting to Lorentzian peaks using the procedure described above. Plots of peak intensity versus time were then fit to a single-exponential decay.

Base-Pair Opening Dynamics: Theory. Imino proton exchange can be modeled as a two-state process:

$$\underset{\text{(closed state)}}{\mathrm{A{:}}H\mathrm{T}} \underset{k_{cl}}{\overset{1/\tau_0}{\rightleftharpoons}} \underset{\text{(open state)}}{\mathrm{A} + H\mathrm{T}} \xrightarrow{k_{ex,open}} \mathrm{A} + H'\mathrm{T}$$

$$K_D = 1/(\tau_0 k_{cl}) \quad (3)$$

where τ_0 is the base-pair lifetime, k_{cl} is the closing rate constant, $k_{ex,open}$ is the rate constant for exchange of the imino proton in the open state, and H is the exchangeable imino proton. For a stable base pair ($K_D \ll 1$), the exchange lifetime of the imino proton at a particular exchange catalyst concentration, τ_{ex}, is given by

$$\tau_{ex} = \tau_0 + 1/k_{ex,open}K_D \quad (4)$$

The catalyst concentration, [cat], is proportional to $k_{ex,open}$ so that a plot of τ_{ex} versus 1/[cat] affords a straight line that extrapolates to τ_0 at infinite [cat] (Guéron & Leroy, 1995).

Within each triplet of pyr·pur-pyr triple helices, there exist both a Watson−Crick and a Hoogsteen base pair. For these imino protons, there are many possible exchange mechanisms, involving different open and closed states. The two-state model divides these configurations into two categories; those that lead to detectable imino proton exchange constitute

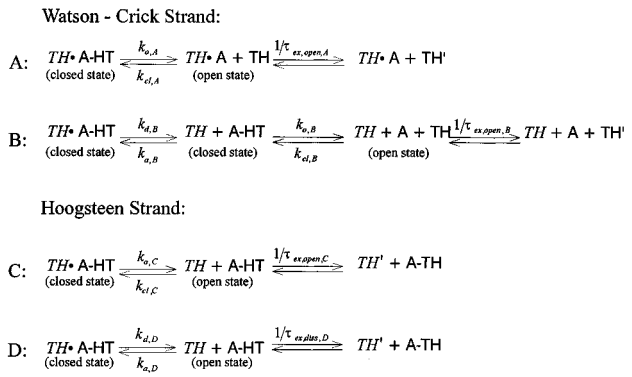

FIGURE 2: Possible exchange mechanisms for the Watson−Crick and the Hoogsteen imino protons. A T·A-T base triplet is taken as an example. The Hoogsteen nucleotide is in italics. Mechanism A represents opening of a Watson−Crick base pair with the Hoogsteen base pairing intact. Mechanism B represents opening of the Watson−Crick base pair after the Hoogsteen strand (in whole or in part) has dissociated. Mechanism C represents opening of a Hoogsteen base pair with Watson−Crick base pairing intact. Mechanism D represents Hoogsteen base-pair opening via dissociation of the Hoogsteen strand.

the open state, and all others correspond to the closed state. Several possible exchange mechanisms are presented in Figure 2. It is possible that the Watson−Crick pairs open from within closed triplets (mechanism A), or they may open only after the Hoogsteen strand has dissociated (mechanism B). The Hoogsteen pairs may open individually within triplets (mechanism C) or cooperatively by dissociation of part of or the entire Hoogsteen strand (mechanism D). Certainly, there are additional possible mechanisms, but these mechanisms can fit into the two-state (closed state and open state) formalism represented by eqs 3 and 4, provided that K_D and τ_0 are redefined. In the case of complex, multistep mechanisms such as mechanism B of Figure 2, the values of τ_0 cannot be interpreted directly as individual rate constants, but the experimentally determined values of τ_0 will retain their meaning as the average lifetimes of the closed states.

In duplex DNA, it is known that imino protons exchange by a two-state model with a single mode of base-pair opening being responsible for all the measured exchange, but that assumption cannot be made here (Guéron et al., 1987). If there are two or more exchange mechanisms for which τ_0 and $\tau_{ex,open}$ differ, then one mechanism could dominate ^{1}H exchange at low [cat] and another could dominate exchange at high [cat]. In such a case, the two-state model presented above may not hold for triplexes. The decision about whether the two-state model applies can only be made by judging whether the plots of τ_{ex} versus 1/[cat] are linear (Leroy et al., 1985).

RESULTS

NOESY Spectra. The imino proton assignments of both **1** and **2** were reported previously (Osborne et al., 1997). The imino protons of base pairs 8 and 7′ exhibit cross-peaks in the NOESY spectrum of **1** and **2** (τ_m = 100 ms, pH 6.0, 1 °C) that correlate with low-intensity peaks in the one-dimensional imino proton spectrum (peaks marked with an × in Figures 3 and 4). For these resonances, the intensity of the cross-peaks far exceeds that of the diagonal peaks. This finding is consistent with a conformational equilibrium

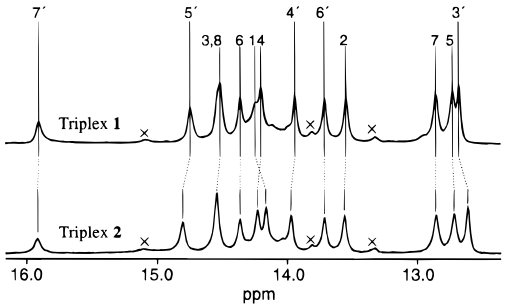

FIGURE 3: 500 MHz NMR spectra of **1** and **2** (pH 6.0 and 1 °C). The resonances are labeled with the number of the base pair containing the imino proton.

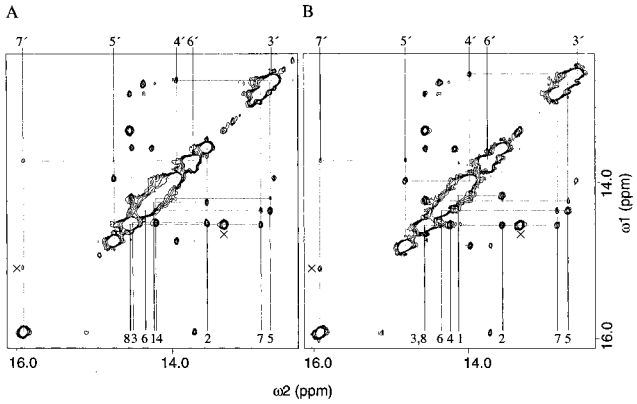

FIGURE 4: NOESY spectral expansions containing the imino proton to imino proton cross-peaks (τ_m = 100 ms, 1 °C). The NOE connectivities involving the Hoogsteen imino protons are delineated above the diagonal, and the connectivities involving the Watson−Crick imino protons are delineated below the diagonal. The resonances are labeled with the number of the base pair containing the imino proton. The peaks marked with an × are exchange peaks due to conformational heterogeneity and are discussed in the text: (A) triplex **1** and (B) triplex **2**.

involving the terminal two triplets in which the low population conformer substantially converts to the predominant conformer in less than 100 ms. Integration of the peaks of interest shows that for both base pairs, the major conformer is present at an approximately 5-fold excess over the minor conformer. There are two additional minor peaks at 13.82 and 14.12 ppm present in the one-dimensional spectrum of **1** and **2**. The peak at 13.82 ppm exhibits an exchange cross-peak close to the diagonal with the 6′ imino protons. Significantly, these minor peaks in **1** and **2** are identical in both intensity and position which indicates that the cross-link does not alter these dynamic processes of the triplex.

Examination of the NOESY spectrum of **1** acquired at pH 6.0 and 37 °C (Figure 5) reveals extensive conformational heterogeneity. The cross-peaks that are boxed in this figure are the peaks expected of the sequential imino proton NOE connectivities from the triplex structure. The remaining cross-peaks (labeled ×) cannot represent transfer between the major diagonal peaks (labeled at the top of the spectrum) because they are only aligned with a major peak in one dimension. Thus, these peaks demonstrate the presence of significant conformational heterogeneity along the melting pathway of **1**. Some of these peaks may represent exchange cross-peaks with a very low population duplex form, but others appear not to be. For example, the imino proton of base pair 4 exhibits a cross-peak (labeled ×*) with a

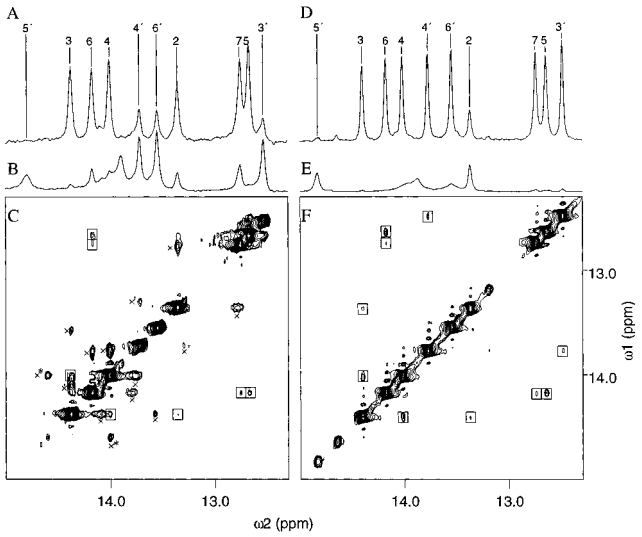

FIGURE 5: NOESY spectral expansions of the imino proton region (τ_m = 100 ms, 37 °C). Panels A and D are one-dimensional projections of the spectral region shown for **1** and **2**, respectively. Panels B and E are vectors at the ω1 frequency of H_2O that represent transfer from H_2O to the imino protons of **1** and **2**, respectively. Panels C and F are the NOESY expansions for **1** and **2**, respectively. The peaks enclosed by boxes arise from sequential NOEs among the imino protons of the triplexes. This network of NOEs is delineated in Figure 4 for the spectra of both molecules at 1 °C. The peaks marked with an × are due to conformational heterogeneity as explained in the text.

resonance that is downfield of any of the duplex resonances noted in previous studies at pH 7.4 and 8.0 (Osborne et al., 1997), and the imino proton of Hoogsteen base pair 4′ exhibits a cross-peak (labeled ×†), although the Hoogsteen base pairs do not exist in the duplex form. Examination of peaks in the NOESY vector at the ω-1 frequency of the water resonance (Figure 5B) reveals considerable transfer of magnetization between H_2O and most of the imino protons of **1**. While these peaks can arise via NOE and/or proton exchange, the fact that many of these peaks are greater in intensity than the diagonal peaks suggests that considerable exchange is occurring among all Hoogsteen and many of the Watson−Crick imino protons. The simultaneous existence of three efficient magnetization transfer pathways (NOE, chemical exchange, and conformational exchange) evident in this spectrum makes a more precise interpretation of these peaks impossible. Importantly, the cross-peaks between the triplex imino resonances and the water protons should not be considered evidence of fast exchange between the triplex protons and water, because the peaks may arise due to a multistep transfer pathway involving a chemical exchange of water protons into the duplex form followed by a duplex to triplex conversion.

The imino proton melting spectra of **2** at pH 6.0 are similar to those of **1**. However, examination of the imino proton to imino proton region of the NOESY spectrum of **2** acquired at 37 °C (Figure 5F) reveals only cross-peaks representing the sequential connectivities of the triplex structure. Thus, for sequence **2**, the cross-link inhibits the conformational heterogeneity that is observed in the spectrum of **1** at 37 °C.

*Exchange Measurements of Sequence **1***. The exchange lifetimes of the imino protons of **1** as a function of pH in the absence of added catalyst were measured by real-time exchange experiments (Table 1). The longest exchange times among the Watson−Crick imino protons are ca. 1 h and occur at pH 5.8 where the triplex form greatly predominates. At this pH, measurable exchange lifetimes are exhibited by the Hoogsteen imino protons from base pairs 4′ and 6′ (dT·dA base pairs) and the hydrogen-bonded amino protons from the Hoogsteen cytosines of base pairs 5′ and 7′. The lifetimes of the cytosine imino protons of base pairs 5′ and 7′ were too short to measure in these experiments. At higher pH values, all the Hoogsteen imino and amino proton lifetimes are less than ∼180 s and cannot be accurately quantified. Curiously, the longest imino proton exchange lifetime for base pair 5 is measured at pH 6.4. It may be that acid-catalyzed proton exchange becomes more efficient at pH 5.8. Acid-catalyzed exchange of guanine imino protons has been noted elsewhere (Nonin et al., 1996).

Table 1: Proton Exchange Lifetimes (s) at 1 °C as a Function of pH for Sequence **1** in PBS Buffer (90% H_2O/10% D_2O) with $MgCl_2$ (0.5 mM)[a]

imino proton	base-pair type	pH 5.8	pH 6.4	pH 6.9
1	T-A	−	−	−
2	G-C	−	−	−
3	A-T	951	475	252
4	A-T	3766	3477	240
5	G-C	3153	3936	3099
6	A-T	2955	2029	−
7	G-C	1984	1559	230
8	A-T	−	−	−
3′	T·A	−	−	−
4′	T·A	306	−	−
5′	C^+·G	990†	−	−
6′	T·A	860	−	−
7′	C^+·G	490†	−	−

[a] The values marked with a † indicate amino proton exchange. The remaining values represent imino proton exchange. The Watson−Crick base pairs are indicated with a hyphen (−) and the Hoogsteen base pairs are indicated with a dot (·). A dash indicates that the exchange lifetimes were too low to be detected by real-time exchange experiments (i.e., less than ca. 180 s).

A significant population of the duplex conformer of **1** is expected at pH 6.9, which is only 0.2 pH unit below the pK_a of cytosine residues in **1** (Völker et al., 1997). Consistent with this expectation, two weak peaks from this duplex conformer are seen in the pH 6.9 spectrum (indicated with an * in Figure 6). The remaining peaks from the duplex conformer overlap and cannot be unambiguously identified. The presence of this equilibrium concentration of duplex conformer does not present any difficulty in determining the exchange times of the triplex protons, because duplex imino protons exchange quickly (<1 s) and are fully exchanged before the first spectrum is measured (ca. 1 min after mixing). Therefore, when the final spectrum of the fully exchanged sample is subtracted from the spectra acquired during exchange, the duplex imino peaks cancel completely.

The imino proton lifetimes of **1** could reflect a combination of exchange from within the triplex and exchange upon conversion to the duplex; i.e., exchange could occur via mechanisms A and B of Figure 2. Estimated integrals for the duplex peaks, marked with asterisks in Figure 6B, lead to the conclusion that at least 17% of the equilibrium population of **1** at pH 6.9 is duplex form. The existence of a Watson−Crick imino proton lifetime as high as 3099 s in

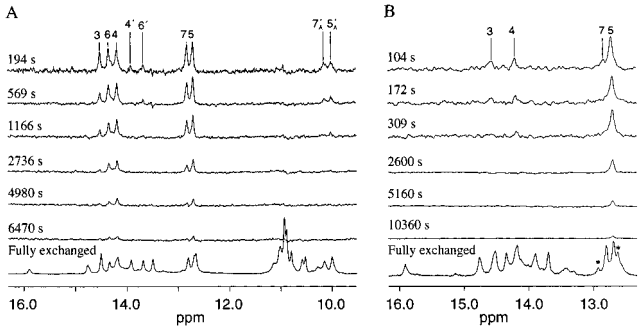

FIGURE 6: Imino and amino proton spectra for **1** as a function of exchange time and pH measured at 1 °C. Real-time exchange spectra were collected as explained in Materials and Methods. The time indicated on each spectrum is the midpoint of the coadded FIDs that comprise the spectrum. The signal to noise increases in successive spectra because more FIDs were coadded to produce the spectra at longer exchange times. The peaks labeled $7'_A$ and $5'_A$ are resonances of amino protons from the cytosines of base pair 7′ and 5′, respectively. All the remaining peaks are imino proton peaks from the base pairs indicated. The peaks labeled with an * are due to a minor population of the duplex conformation: (A) pH 5.8 and (B) pH 6.9.

the presence of a substantial equilibrium duplex population indicates that the triplex to duplex conversion rate is very slow in comparison to the rate of Watson−Crick imino proton exchange from within a duplex (<1 s). Therefore, the Watson−Crick imino protons of **1** will exchange with nearly every triplex to duplex conversion under these conditions, and the measured exchange rate ($1/\tau_{ex}$) for the base pair 5 imino proton at pH 6.9 (3.2×10^{-4} s^{-1}) should be considered an upper bound for the rate of triplex to duplex conversion under the conditions of these measurements.

*Exchange Measurements of Sequence **2***. The base-pair lifetimes of **2** were characterized by measuring imino and amino proton exchange lifetimes as a function of exchange catalyst concentration and temperature at pH 7.8. These experiments could not be conducted for **1** because this sequence exists predominately in the duplex state at the high pH necessary for efficient exchange catalysis used in these measurements. Without added catalyst, the imino proton exchange times at 1 °C can be measured in real-time exchange experiments (Table 2). The exchange times measured in the absence of added catalyst are higher than any measured for **1** despite being measured at a higher pH, and the highest exchange lifetimes tend to be in the middle of the triplex.

Line broadening of the imino resonances of base pairs 1, 2, and 3′ is clearly evident due to enhanced proton exchange catalyzed by the unprotonated form of the TRIS buffer (Figure 7). The broadening of the base pair 1 and 2 imino protons is not surprising because these base pairs seem to fray early in the melting profiles (Osborne et al., 1997) of **2**, and therefore, enhanced exchange is suspected. The broadening of the base pair 3′ imino proton is less expected because it is not seen in the melting profile of **2**. Interestingly, the base pair 3′ imino proton of **1** is exchange broadened at pH 7.4 and 1 °C. Thus, the fraying pattern observed for **1** is reflected in **2**, but only after the addition of added exchange catalyst.

The imino proton of base pair 5′, which is substantially exchange broadened without added catalyst at 21 and 38 °C, does not broaden further upon addition of exchange catalyst

Table 2: Imino Proton Exchange Lifetimes, τ_{ex}, and Base-Pair Lifetimes, τ_0, of Sequence **2** as a Function of Temperature at pH 7.8[a]

imino proton	base-pair type	τ_{ex} (s) 1 °C	τ_0 (ms) 21 °C	τ_0 (ms) 38 °C
1	T-A	0	<3	m
2	G-C	0	27	<3
3	A-T	1016	69[b]	6
4	A-T	3748	184	27
5	G-C	6342	−	232
6	A-T	1865	36[b]	21
7	G-C	1460	104	14
8	A-T	m	m	m
2′	C^+·G	m	m	m
3′	T·A	0	<3	<3
4′	T·A	2437	10	<3
5′	C^+·G	2113[c]	126[d]	34[d]
6′	T·A	1499	67	6
7′	C^+·G	276[c]	m	m
8′	T·A	m	m	m

[a] Both the Watson−Crick and Hoogsteen base-pair lifetimes (τ_0) are greatest in the middle of the sequence and decrease near the termini. In every case measured, the lifetime of the Watson−Crick base pair exceeds that of the Hoogsteen base pair which is contained in the same triplet. The exchange lifetimes were measured in PBS buffer (90% H_2O/10% D_2O) with $MgCl_2$ (0.5 mM), while the base-pair lifetimes were measured in the presence of an increasing TRIS catalyst concentration. Resonances that were too exchange broadened for measurement are indicted with an m. Resonances for which the T_1 value did not change sufficiently for accurate measurement are indicated with a dash (−). Generally, this means that the resonances exhibit long exchange lifetimes (i.e., ca. 300 ms). Resonances for which overlap is too severe are designated ovr. [b] All errors are under 25% except for these resonances. [c] These exchange times are for the amino proton of the cytosine in this base pair. [d] These values of τ_o are estimated directly from the T_1 values (see the text).

(Figure 7). The remaining Hoogsteen imino protons, 3′, 4′, and 6′, exhibit a far different response to exchange catalyst. At 38 °C, the 3′, 4′, and 6′ protons exhibit narrow resonances in the absence of added catalyst, but these resonances nearly broaden into the baseline upon addition of catalyst. This finding indicates that the exchange rate for the base pair 5′ imino proton, in contrast to those of the other Hoogsteen protons, at 21 and 38 °C is not catalyst-dependent. This could result from particularly efficient exchange from the protonated cytosine, which in the open state may exhibit a pK_a value similar to that of an isolated cytosine (pK_a = 5.5; Singleton & Dervan, 1992).

Upon addition of TRIS catalyst (12.7 mM), all the imino proton exchange lifetimes become too short to be measured in real-time experiments (<180 s). Therefore, the exchange times of these imino protons in the presence of added catalyst were determined by measuring the selective T_1 times of the imino proton resonances as a function of exchange catalyst concentration. The exchange lifetimes of the more slowly exchanging imino protons could not be determined, because exchange lifetimes much greater than the T_1 values measured in the absence of added catalyst but shorter than 180 s cannot be obtained with this technique (Guéron & Leroy, 1995). Plots showing the variation of imino proton exchange time (τ_{ex}) with inverse catalyst concentration at 21 and 38 °C are presented in Figure 8, and the extrapolated values of τ_0 are given in Table 2. The most complete data set is achieved for exchange at 38 °C, because the exchange rates are generally fast enough to be measured at this temperature.

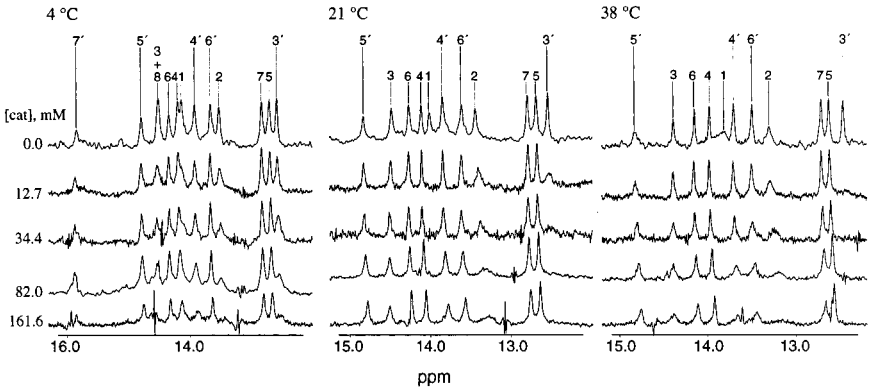

FIGURE 7: Imino proton region of 500 MHz NMR spectra of **2** as a function of TRIS exchange catalyst concentration at pH 7.8 in PBS buffer (90% H_2O/10% D_2O) with $MgCl_2$ (0.5 mM). The peaks are labeled according to the nomenclature introduced in Figure 1.

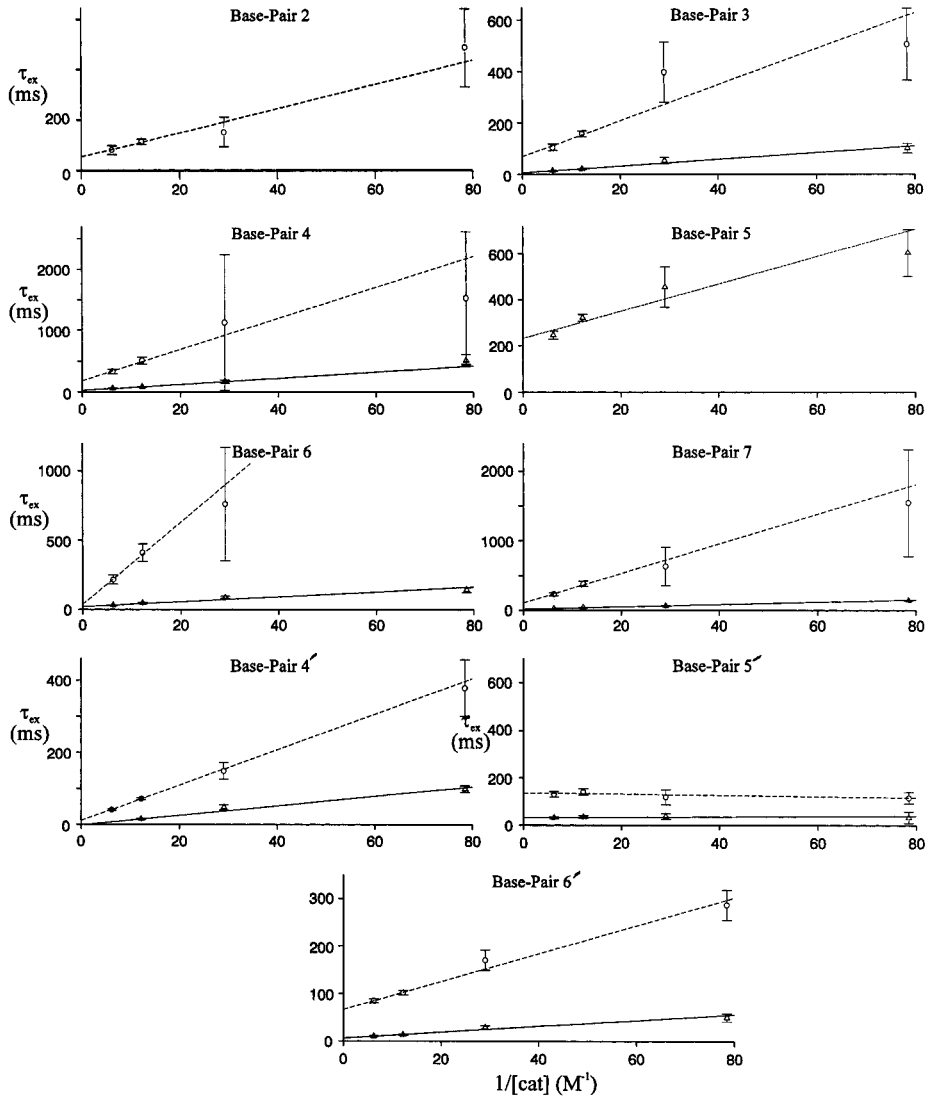

FIGURE 8: Variation of imino proton exchange time with inverse catalyst concentration. The data markers and fitting lines are designated as follows: Dashed lines and open circles indicate 21 °C, and solid lines and open triangles indicate 38 °C. The curves are straight lines fit to the data and weighted according to the error. The error bars indicate the propagated errors from the T_1 measurements. Not all imino proton exchange times could be measured under all conditions (see the text for details).

The melting temperature of **2** as determined by UV measurements conducted under solution conditions similar to those used in these NMR studies (without catalyst) is 47 °C which raises the possibility that some of the exchange measured at 38 °C may result from thermal denaturation rather than from internal modes of base-pair opening. However, a cooperative melting process, such as occurs with this triplex, should yield uniform values of τ_0, whereas a large range of τ_0 values were measured here.

The variation of longitudinal relaxation time with temperature and catalyst concentration is unique for the cytosine imino proton of base pair 5′. At 21 and 38 °C, the

longitudinal relaxation time of this proton is invariant with respect to increased catalyst concentration. This behavior could result from two circumstances: Either the imino protons exchange too slowly to effect these measurements, or the exchange is fast and not dependent on catalyst concentration because exchange occurs with each opening event even in the absence of catalyst. Several lines of evidence point to the latter alternative. First, the melting spectra for **2** (Osborne et al., 1997) reveal that the 5′ imino proton broadens at a much lower temperature compared to most of the protons and is severely broadened at 40 °C and pH 7.4, in the absence of added catalyst. Second, the 5′ imino proton resonance of **2** does not move upfield upon melting (Osborne et al., 1997) as do all the remaining imino protons. Imino protons shift upfield during melting because of an equilibrium between closed and open states, but when exchange occurs every time the base pair opens, then no upfield shift can occur because the same proton will not exchange back from water. Third, the measured values of T_1 for the 5′ proton at 21 and 38 °C are far below that of the other stable base pairs (see the Supporting Information) which is consistent with fast exchange causing fast longitudinal relaxation. For the T_1 of the 5′ imino proton of **2** to be both dominated by proton exchange and independent of exchange catalyst concentration, exchange for this proton should be opening-rate limited.

The exchange lifetimes of the 5′ imino proton at 21 and 38 °C are therefore estimated directly from the longitudinal relaxation time because exchange dominates the measured T_1 values. Furthermore, because under these conditions exchange is opening-rate limited and therefore independent of exchange catalyst concentration, the τ_0 values reported in Table 2 for base pair 5′ at 21 and 38 °C are the average of the exchange lifetimes at various catalyst concentrations.

DISCUSSION

Base-Pair Opening Dynamics. The base-pair opening dynamics in duplex DNA has been the subject of intensive investigation. A motivating factor behind these experiments is that base-pair opening is implicated in a number of important chemical, biological, and mechanical processes that involve DNA (Ramstein & Lavery, 1988, 1990; Frank-Kamenetski, 1985; Tari & Secco, 1995). Previous work has established that within duplex DNA, base pairs can open individually and that base-pair opening is sensitive to structural perturbations. However, the base-pair opening dynamics of triplex DNA has not been reported. Thus, it is not known whether the base pairs (Hoogsteen and Watson−Crick) that comprise the triplets of triple-helical DNA open to any significant extent within a stable triplex.

Small intermolecular triple helices that contain cytosine residues in the Hoogsteen strand exhibit apparent pK_a values of ∼5.5, and intramolecular cytosine-containing triplexes exhibit pK_a values of up to 7.0 (Singleton & Dervan, 1992). Thus, for pyr·pur-pyr triple helices, such measurements are not possible because base-pair lifetimes can only be measured at alkaline pH to have efficient imino proton exchange. At such pH values, most triplexes containing Hoogsteen strand cytosines are conformationally labile. The studies described here along with work described elsewhere have shown that sequence **2** is remarkably stable and homogeneous under a variety of solution conditions and at relatively high temperatures (Osborne et al., 1997; Völker et al., 1997). Thus, cross-linked triplex **2** is an ideal construct for measuring base-pair opening dynamics.

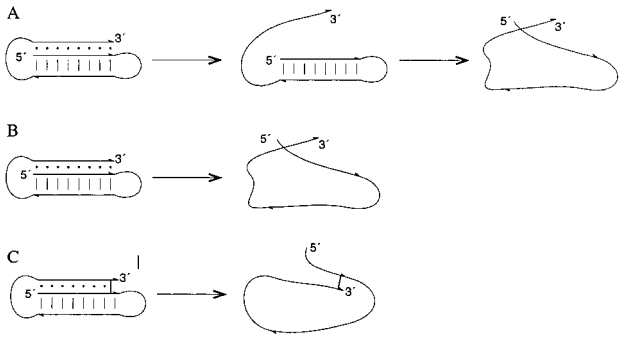

FIGURE 9: Schematic presentation of the thermal denaturation pathways apparently exhibited by **1** and **2**. Watson−Crick and Hoogsteen base pairs are designated by vertical lines (|) and dots (·), respectively. The disulfide cross-link is designated by a thick line linking different parts of the strand. The 5′ and 3′ ends of the strands are indicated. (A) The pathway exhibited by **1** at pH 7.4 and 8.0. An initial denaturation from the triplex to the duplex conformation is followed by a duplex to single-strand conversion. (B) The predominate pathway exhibited by **1** at pH 6.0. The triplex denatures directly to the single-strand conformation. While this appears to be the predominate pathway for this denaturation, there may be significant populations of intermediate conformers as explained in the text. (C) The pathway exhibited by **2** at each pH studied. The triplex denatures in an apparently two-state manner with no evidence of intermediate structures.

Effect of the Cross-Link on Conformational Heterogeneity. NOESY spectra of **2** measured at pH 6.0 and 37 °C clearly show that the cross-link suppresses the conformational heterogeneity observed in **1** under the same conditions. This observation is consistent with UV thermal denaturation and calorimetric studies which indicate that **1** melts directly from triplex to single strand at pH values below 5.75, but melts from triplex to duplex to single strand at a pH value above 6.25. Thus, the pH range from 5.75 to 6.25 represents a "gray area" for the melting of **1** where significant populations of triplex, duplex, and single strand may coexist. On the basis of UV melting curves acquired under solution conditions similar to those used in the NMR experiments, we estimate that **1** is approximately 5−10% denatured at 37 °C.

Effect of the Cross-Link on Proton Exchange Dynamics. The real-time exchange results presented in Tables 1 and 2 reveal that for both **1** and **2**, the presence of the Hoogsteen strand profoundly affects the exchange kinetics of the Watson−Crick base pairs. Rates of third strand dissociation vary dramatically with sequence length, composition, and temperature (Xodo, 1995; Shindo et al., 1993; Bates et al., 1995; Yang et al., 1994; Kang et al., 1992; Wang et al., 1995), but tend to be low, often on the order of h^{-1}. In this context, the slow rate of triplex to duplex conversion noted for **1** ($k \leq 3.2 \times 10^{-4}$ s^{-1}) is not surprising. However, there must be efficient mechanisms for the Hoogsteen imino protons of **1** to exchange from within the triplex at pH 6.9 because these exchange rates far exceed the upper bound for the rate of triplex to duplex conversion.

The Watson−Crick imino proton exchange lifetimes of **2** measured in the absence of added catalyst are somewhat longer than those for **1** despite a higher pH. Surprisingly, given the fact that the Hoogsteen imino and amino protons

of **1** at pH 6.9 exchange efficiently from within the triplex, these protons in **2** at pH 7.6 exchange with lifetimes greater than 1500 s for base pairs 4′, 5′, and 6′. Whether this added exchange stability is due to a dynamic effect of the cross-link or to an effect of the increased pH on the exchange dynamics of the triplex is unclear.

Upon the first addition of TRIS to **2**, all the base-pair lifetimes become too short to be measured with real-time exchange experiments (<180 s) which indicates that the rate-limiting step in imino proton exchange is not base-pair opening. As mentioned earlier, the assumption that exchange occurs via the same mechanism at all catalyst concentrations can be assessed by judging the linearity of τ_{ex} versus 1/[cat] plots. The condition of linearity seems to be satisfied here in most cases. However, in several cases, it is possible that two separate mechanisms may be involved. For example, the exchange plots for base pairs 3 and 4 at 21 °C and base pair 5 at 38 °C may be linear but are also consistent with two mechanisms (Figure 8). If that is the case, then the values of τ_0 reported in Table 2 will be greater than the true base-pair lifetime, i.e., $[(1/\tau_{0,\text{mechanism1}}) + (1/\tau_{0,\text{mechanism2}})]^{-1}$, and thus could be considered an upper limit for the base-pair lifetimes.

The base-pair lifetimes measured at 38 °C are longer than would be seen in duplex DNA, indicating that the Hoogsteen strand in the major groove stabilizes these base pairs against opening. Luzopeptin and chromomycin, two drugs that bind in the minor groove of duplex DNA, extend Watson−Crick base-pair lifetimes to a similar extent (Leroy et al., 1991, 1992). Thus, binding in either groove can have a similar effect.

Previous studies of duplexes have shown that base pairs not involved in terminal fraying can open individually, even in complexes with minor groove binding drugs (Leroy et al., 1991, 1992). This conclusion was based on the nearly random distribution of base-pair lifetimes among neighboring base pairs (Guéron & Leroy, 1995). Such a distribution of base-pair lifetimes is not noted for triplex **2**. Base pair 5, located in the center of triplex **2**, exhibits the longest base-pair lifetime, and values taper off toward both termini. In fact, the pattern of high base-pair lifetimes in the middle of the triplex, which is also noted at 21 and 4 °C, suggests that end effects may be impacting the exchange process. Such end effects could be due to fraying or to some residual conformational heterogeneity at the termini that is not suppressed by the cross-link. Even at low pH and temperature, conformational heterogeneity has been noted in NMR studies of other triplexes (Sklenár & Feigon, 1990). Both **1** and **2** exhibited identical evidence of conformational heterogeneity at the 8 and 8′ termini at 1 °C and pH 6.0. While this heterogeneity did not seem to increase with temperature for **2** as it did for **1**, it is possible that this heterogeneity is a significant factor in imino proton exchange for both triplexes. Further studies with longer triplexes could clarify this point.

CONCLUSIONS

The experiments described here represent the first measurement of the lifetimes of Hoogsteen base pairs. Similar to those of Watson−Crick base pairs, the Hoogsteen lifetimes are highest at the centrally located region within the triplex and taper off toward the termini, which is consistent with imino exchange mechanisms that may involve end effects. In all cases, the lifetime of a Hoogsteen base pair is shorter than that of the Watson−Crick base pair contained in the same triplet, and is consistent with the greater stability of Watson−Crick compared to Hoogsteen base pairs (Plum et al., 1995). The rate of triplex to duplex conversion for **1** at 1 °C and pH 6.9 is low with an upper bound of 3.2×10^{-4} s^{-1}. The imino protons of **2** exchange slowly in PBS with exchange times as long as 1 h, but the base-pair lifetimes are all less than 3 min, reflecting the fact that imino proton exchange is not opening-rate limited. At 21 and 38 °C, all but one of the base-pair lifetimes are less than 250 ms. With the data reported here, the structure, dynamics, and thermodynamic stability of **1** and **2** have been addressed. Taken together, these data provide a reasonably thorough understanding of the factors that govern the structure and stability of this sequence. In addition, these experiments demonstrate the utility of our disulfide chemistry in studies of nucleic acid chemistry and biophysics.

SUPPORTING INFORMATION AVAILABLE

Imino proton longitudinal relaxation times measured as a function of exchange catalyst concentration and temperature (1 page). Ordering information is given on any current masthead page.

REFERENCES

Bates, P. J., Dosanjh, H. S., Kaman, S., Jenkins, T. C., Laughton, C. A., & Neidle, S. (1995) *Nucleic Acids Res. 23*, 3627−3632.

Cain, R. J., & Glick, G. D. (1997) *Nucleic Acids Res. 25*, 836−842.

Dervan, P. B. (1992) *Nature 359*, 87−88.

Ernst, R. R., Bodenhausen, G., & Wokaun, A. (1987) *Principles of Nuclear Magnetic Resonance in One and Two Dimensions*, Oxford University Press, New York.

Felsenfeld, G., Davies, D. R., & Rich, A. (1957) *J. Am. Chem. Soc. 79*, 2023−2024.

Folta-Stogniew, E., & Russu, I. M. (1996) *Biochemistry 35*, 8439−8449.

Frank-Kamenetski, M. D. (1985) in *Structure and Motion: Membranes, Nucleic Acids, and Proteins* (Clementi, E., Corongiu, G., & Sarma, M. H., Sarma, R. H., Eds.) pp 417−432, Adenine Press, Guilderland, NY.

Geen, H., & Freeman, R. (1991) *J. Magn. Reson. 93*, 93−141.

Guéron, M., & Leroy, J. L. (1995) *Methods Enzymol. 261*, 383−413.

Guéron, M., Kochoyan, M., & Leroy, J. L. (1987) *Nature 328*, 89−92.

Günther, H. (1995) *NMR Spectroscopy*, pp 346−348, John Wiley & Sons, Chichester, England.

Heider, A. R., & Bardos, T. J. (1995) in *Cancer Chemotherapeutic Agents* (Foye, W. O., Ed.) pp 529−576, American Chemical Society, Washington, DC.

Kang, S., Wohlrab, F., & Wells, R. D. (1992) *J. Biol. Chem. 267*, 19435−19442.

Leroy, J. L., Bolo, N., Plateau, P., & Guéron, M. (1985) *J. Biomol. Struct. Dyn. 2*, 915−939.

Leroy, J. L., Kochoyan, M., Huynh-Dinh, T., & Guéron, M. (1988) *J. Mol. Biol. 200*, 223−238.

Leroy, J. L., Gao, X. L., Guéron, M., & Patel, D. J. (1991) *Biochemistry 30*, 5653−5661.

Leroy, J. L., Gao, X. L., Misra, V., Guéron, M., & Patel, D. J. (1992) *Biochemistry 31*, 1407−1415.

Macaya, R., Wang, E., Schultze, P., Sklenár, V., & Feigon, J. (1992) *J. Mol. Biol. 225*, 755−773.

Mirkin, S. M., & Krank-Kamenetskii, M. D. (1994) *Annu. Rev. Biophys. Biomol. Struct. 23*, 541−576.

Moser, H. E., & Dervan, P. B. (1987) *Science 238*, 645−650.

Nonin, S., Leroy, J. L., & Guéron, M. (1996) *Nucleic Acids Res. 24*, 586−595.

Osborne, S. E., Cain, R. J., & Glick, G. D. (1997) *J. Am. Chem. Soc. 119*, 1171−1182.
Plateau, P., & Guéron, M. (1982) *J. Am. Chem. Soc. 104*, 7310−7311.
Plum, G. E., Pilch, D. S., Singleton, S. F., & Breslauer, K. J. (1995) *Annu. Rev. Biophys. Biomol. Struct. 24*, 319−350.
Radhakrishnan, I., & Patel, D. J. (1993) *Structure 1*, 135−152.
Radhakrishnan, I., & Patel, D. J. (1994a) *Structure 2*, 17−32.
Radhakrishnan, I., & Patel, D. J. (1994b) *Structure 2*, 395−405.
Radhakrishnan, I., & Patel, D. J. (1994c) *J. Mol. Biol. 241*, 600−619.
Radhakrishnan, I., Gao, X., de los Santos, C., Live, D., & Patel, D. J. (1991) *Biochemistry 30*, 9022−9030.
Ramstein, J., & Lavery, R. (1988) *Proc. Natl. Acad. Sci. U.S.A. 85*, 7231−7235.
Ramstein, J., & Lavery, R. (1990) *J. Biomol. Struct. Dyn. 7*, 915−933.
Shindo, H., Torigoe, H., & Sarai, A. (1993) *Biochemistry 32*, 8963−8969.
Singleton, S. F., & Dervan, P. B. (1992) *Biochemistry 31*, 10995−11003.
Slenár, V., & Feigon, J. (1990) *Nature 345*, 836−838.
Soyfer, V. N., & Potaman, V. N. (1996) *Triple-Helical Nucleic Acids*, Springer-Verlag, Berlin.
Sun, J., Garestier, T., & Hélène, C. (1996) *Curr. Opin. Struct. Biol. 6*, 327−333.
Tari, L. W., & Secco, A. S. (1995) *Nucleic Acids Res. 23*, 2065−2073.
Thuong, N. T., & Hélène, C. (1993) *Angew. Chem., Int. Ed. Engl. 32*, 666−690.
Völker, J., Osborne, S. E., Glick, G. D., & Breslauer, K. J. (1997) *Biochemistry 36*, 756−767.
Wang, S., Friedman, A. E., & Kool, E. T. (1995) *Biochemistry 34*, 9774−9784.
Xodo, L. E. (1995) *Eur. J. Biochem. 228*, 918−926.
Yang, M., Ghosh, S. S., & Millar, D. P. (1994) *Biochemistry 33*, 15329−15337.

BI971342T